ELSEVIER

Journal of Hepatology 44 (2006) 1046–1054

Journal of Hepatology

www.elsevier.com/locate/jhep

In vivo hepatic HB-EGF gene transduction inhibits Fas-induced liver injury and induces liver regeneration in mice: A comparative study to HGF

Ngin Cin Khai[1,2], Tomoyuki Takahashi[1,3,5], Hiroaki Ushikoshi[1,2], Satoshi Nagano[1,4,5], Kentaro Yuge[1], Masayasu Esaki[1,2], Takao Kawai[1,2], Kazuko Goto[1,2], Yoshiteru Murofushi[1,5], Takako Fujiwara[6], Hisayoshi Fujiwara[2], Ken-ichiro Kosai[1,4,5,*]

[1]*Department of Gene Therapy and Regenerative Medicine, Gifu University School of Medicine, Gifu University Graduate School of Medicine, Gifu, Japan*
[2]*Department of Cardiology, Respiratory and Nephrology, Regeneration and Advanced Medical Science, Gifu University Graduate School of Medicine, Gifu, Japan*
[3]*Department of Advanced Therapeutics and Regenerative Medicine, Kurume University, Kurume, Japan*
[4]*Department of Pediatrics, Kurume University School of Medicine, Kurume University, Kurume, Japan*
[5]*Division of Gene Therapy and Regenerative Medicine, Cognitive and Molecular Research Institute of Brain Diseases, Kurume University, 67 Asahi-machi, Kurume 830-0011, Japan*
[6]*Department of Food Science, Kyoto Women's University, Kyoto, Japan*

***Background/Aims*: It is unknown whether heparin-binding EGF-like growth factor (HB-EGF) can be a therapeutic agent, although previous studies suggested that HB-EGF might be a hepatotrophic factor. This study explores the potential of hepatic HB-EGF gene therapy in comparison with HGF.**

***Methods*: Mice received an intraperitoneal injection of the agonistic anti-Fas antibody 72 h after an intravenous injection of either adenoviral vector (1×10^{11} particles) expressing human HB-EGF (Ad.HB-EGF), human HGF (Ad.HGF) or no gene (Ad.dE1.3), and were sacrificed 24 or 36 h later to assess liver injury and regeneration.**

***Results*: Exogenous HB-EGF was predominantly localized on the membrane, suggesting the initial synthesis of proHB-EGF in hepatocytes. The control Ad.dE1.3-treated mice represented remarkable increases in serum ALT and AST levels and histopathologically severe liver injuries with numerous apoptosis, but a limited number of mitogenic hepatocytes. In contrast, the liver injuries and apoptotic changes were significantly inhibited, but the mitogenic hepatocytes remarkably increased, in both the Ad.HB-EGF- and Ad.HGF-treated mice. More mitogenic hepatocytes and milder injuries were observed in the Ad.HB-EGF-treated mice.**

***Conclusions*: HB-EGF has more potent protective and mitogenic effects for hepatocytes than HGF, at least for the present conditions. In vivo hepatic HB-EGF gene transduction is therapeutic for Fas-induced liver injury.**

***Keywords*: Heparin-binding epidermal growth factor-like growth factor; HB-EGF; Hepatocyte growth factor; HGF; Growth factor; Gene therapy; Apoptosis; Fulminant hepatic failure; Fas; Liver regeneration; Adenoviral vector**

Received 9 February 2005; received in revised form 20 September 2005; accepted 10 October 2005; available online 7 December 2005

* Corresponding author. Address: Division of Gene Therapy and Regenerative Medicine, Cognitive and Molecular Research Institute of Brain Diseases, Kurume University, 67 Asahi-machi, Kurume 830-0011, Japan. Tel.: +81 942 31 7581; fax: +81 942 31 7911.
E-mail address: kosai@med.kurume-u.ac.jp (K.- Kosai).

0168-8278/$32.00
doi:10.1016/j.jhep.2005.10.027

1. Introduction

Certain growth factors act as hepatogenic and hepatotrophic factors and play essential roles in the development and homeostasis of the liver. The hepatotrophic factors that have been well studied are hepatocyte growth factor (HGF), epidermal growth factors (EGF) and transforming growth factor-α (TGF-α); their expressions are found in the adult liver under normal physiological conditions and are drastically upregulated during liver regeneration after a partial hepatectomy or liver injury [1–5]. The knockout of any of these genes in mice led to aplasia or dysmaturation of the liver [6,7], and the overexpression of any of them in the transgenic mice accelerated the proliferation of hepatocytes after a partial hepatectomy [8]. Moreover, several animal studies have shown that HGF can be a potent therapeutic agent for liver disorders by inhibiting hepatocyte apoptosis and/or inducing liver regeneration, regardless of administration of the recombinant protein or the gene therapy strategy used [3,9–16].

Heparin-binding epidermal growth factor-like growth factor (HB-EGF), which was identified as a new member of the EGF-family of growth factors, is also expressed in the normal liver [17,18]. The biologically unique feature of this growth factor is that the membrane-anchored precursor form (proHB-EGF) is initially synthesized and subsequently cleaved at the juxtamembrane domain by a specific metalloproteinase [19–21], and the resultant soluble form (sHB-EGF) represents the potent mitogenic activity for a number of cell types [22,23]. The HB-EGF mRNA levels were rapidly increased in the nonparenchymal cells of the regenerating liver, mainly in Kupffer cells and sinusoidal endothelial cells, but not in hepatocytes, after a 70% partial hepatectomy [24] or after liver injury by hepatotoxins [25]. Interestingly, the increase in HB-EGF mRNA was more rapid than that of HGF mRNA, e.g. their maximal levels were reached at 6 and 24 h after partial hepatectomy, respectively [24], suggesting the distinct role and/or mechanism of HB-EGF in liver regeneration compared to HGF. Moreover, exogenous HB-EGF stimulated the DNA synthesis in rat hepatocytes in in vitro [25] and in vivo experiments [26], and the hepatocyte-specific overexpression of HB-EGF in the transgenic mice accelerated the in vivo proliferation of hepatocytes after a partial hepatectomy [27]. Thus, it is likely that HB-EGF may also be acting as the hepatotrophic factor, probably in the early phase of liver regeneration. However, the therapeutic potential of HB-EGF for liver disorders, e.g. the question of whether exogenous HB-EGF acts to inhibit liver injury, has not yet been studied. Other important points are that the possibility of HB-EGF gene therapy has not yet been studied for any diseases in any organs, including liver diseases, except for our recent study on heart disorders, and that the HB-EGF gene therapy trial for myocardial infarction in rabbits did not exert therapeutic effects but rather exacerbated remodeling [28]. Thus, it is biologically and clinically meaningful to investigate whether HB-EGF gene therapy can be potentially used to treat liver disorders.

In this study, the HB-EGF gene was adenovirally transduced into the mouse liver and its potential to inhibit liver injury and stimulate liver regeneration were investigated. Furthermore, these potentials were simultaneously compared to those of HGF, which is currently the best-studied hepatotrophic and therapeutic factor.

2. Materials and methods

2.1. Recombinant adenoviral vectors

Replication-defective recombinant adenoviral vectors (Ads), Ad.HB-EGF, Ad.HGF, Ad.LacZ and Ad.dE1.3, which express human HB-EGF, human HGF, LacZ and no gene under the transcriptional control of a Rous sarcoma virus long-terminal repeat, were prepared as described previously [28–31].

2.2. Animal studies

The schedule of the experiment on therapeutic potentials is shown in Fig. 2(A). Male 5 to 6 week-old C57BL/6J mice ($n=10$, each group) (Chubu Kagaku, Nagoya, Japan) were given an intravenous injection of 1×10^{11} particles of Ad via a tail vein. 72 h later, they were given an intraperitoneal injection of 4 μg of agonistic anti-mouse Fas monoclonal antibody (Jo-2, Beckton-Dickinson Biosciences, San Jose, CA) [14]. All mice were subsequently sacrificed 24 or 36 h later, and liver and blood samples were collected for examination. On the other hand, in vivo adenoviral gene transduction efficiency or the in situ detection of exogenous human HB-EGF was analyzed using the same dose (1×10^{11} particles) of either Ad.LacZ or Ad.HB-EGF, respectively, in intact mice. All animal studies were performed in accordance with the National Institute of Health guidelines as dictated by the Animal Care Facility at the Gifu University School of Medicine.

2.3. Histopathologic analysis

For histopathological observation, liver tissues were fixed in 10% formalin and embedded in paraffin, and 4-μm sections were cut and stained with hematoxylin and eosin (H-E). For assessing the in vivo adenoviral gene transduction efficiency, *O*-nitrophenyl-β-D-galactophyranoside (x-gal) staining was done using the frozen tissue as described previously [28–31]. For detecting apoptotic cells, a terminal deoxynucleotidyl transferase-mediated deoxyuridine triphosphate biotin nick end labeling (TUNEL) assay (ApopTag kit, Intergen Co., Purchase, NY) was done in accordance with the manufacturer's protocol.

Immunohistochemistry was carried out for in situ detection of the cells expressing the HB-EGF transgene or regenerating hepatocytes. In the former, 6-μm frozen sections were fixed in 4% paraformaldehyde and stained with primary goat anti-human HB-EGF antibody (R&D Systems Inc., Minneapolis, MN), secondary donkey anti-goat IgG Alexa 568 antibody (Molecular Probes, Inc., Eugene, OR), and Hoechst 33342 (Molecular Probes, Inc.). In the latter, the formalin-fixed and paraffin-embedded tissues were deparaffinized and rehydrated, and then heated in 10 mmol/L citrate buffer, pH 6.0 for 10 min for the antigen retrieval. Endogenous peroxidase activity and the non-specific binding of antibody were blocked by 0.3% H_2O_2 and normal rabbit serum. The anti-Ki67 (TEC-3, DakoCytomation, Denmark) primary antibody, biotinylated anti-rat IgG secondary antibody, avidin-peroxidase, diaminobenzidine in hydrogen peroxidase and chromogen were applied in order and were subsequently counterstained with hematoxylin.

Digital images observed with a laser-confocal microscope (LSM510, Carl Zeiss, Oberkochen, Germany) were employed for the morphometric and quantitative analyses using Adobe Photoshop 7.0 software (Adobe Systems Inc., San Jose, CA). Quantitative analyses of the replicating and apoptotic hepatocytes were done as described previously with some modifications [13,15]. Briefly, Ki-67-positive, Ki-67-negative or TUNEL-positive hepatocytes were counted in 30 fields at random under 200×

magnification (approximately 2000 cells in 3 slides per mouse), and the percentages of the replicating hepatocytes and numbers of the apoptotic hepatocytes in a field were calculated.

2.4. Biochemical Analyses

Serum alanine aminotransferase (ALT) and aspartate aminotransferase (AST) levels were measured using a standard clinical automatic analyzer (Hitachi 736) (Hitachi Co. Ltd., Tokyo, Japan) at 24 or 36 h after the anti-Fas antibody injection.

2.5. Statistical Analysis

Data were represented as the means +/− standard errors. Statistical significance was determined using the Student's *t*-test. $P<0.05$ was considered statistically significant.

3. Results

3.1. Adenoviral gene transduction efficiency and HB-EGF transgene expression

In accordance with previous findings [16,32], Ad.LacZ injection and subsequent x-gal staining revealed that an intravenous injection of 1×10^{11} particles of Ad resulted in approximately between 60 and 90% gene transduction in hepatocytes (Fig. 1(A)). Ad.HB-EGF injection and the subsequent immunohistochemistry against the human HB-EGF confirmed this finding. Moreover, the exogenous HB-EGF protein was predominantly observed on the membrane, and the cytoplasm was faintly positive for exogenous HB-EGF. These findings suggest that the initially synthesized exogenous HB-EGF was membrane-anchored proHB-EGF, and that the resultant sHB-EGF by the shedding of proHB-EGF might bind to and activate hepatocytes in the autocrine fashion, followed by the endocytosis of exogenous HB-EGF in hepatocytes.

3.2. Liver enzymes after HB-EGF or HGF gene therapy

Recent studies have suggested that the initial and essential event in acute and/or chronic hepatitis, including fulminant hepatic failure, may be the excessive activation of the Fas system [33,34] and that the administration of the agonistic anti-Fas antibody in mice leads to fulminant hepatic failure [14,35]. As we clearly elucidated the therapeutic effect of HGF in this animal model [14], this model may be suitable to use for the initial examination of the in vivo anti-apoptotic effect on hepatocytes and the

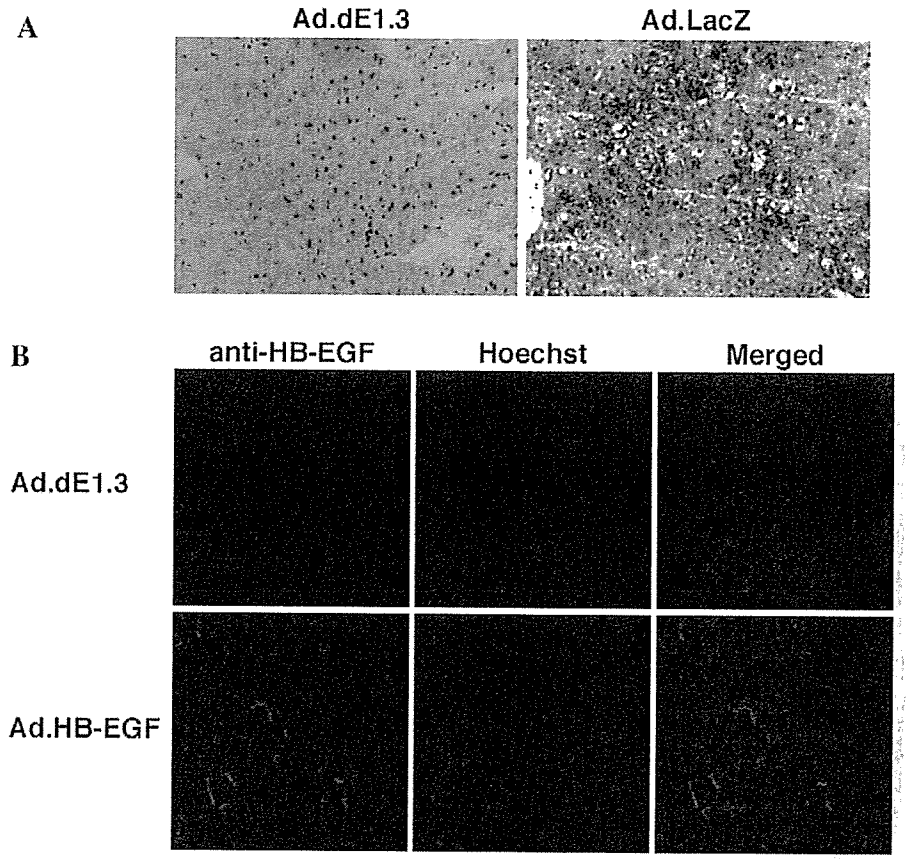

Fig. 1. Adenoviral gene transduction and expression in mice. (A) X-gal staining of the liver 48 h after an intravenous injection of either Ad.LacZ or control Ad.dE1.3 into an intact mouse. (B) Immunohistochemical staining for exogenous human HB-EGF of the liver 48 h after an intravenous injection of either Ad.HB-EGF or control Ad.dE1.3 into an intact mouse.

therapeutic potential of a certain agent for liver disorders. To perform this assessment, we initially injected Ad, and then subsequently injected the anti-Fas antibody 72 h later. We sacrificed the mice 24 or 36 h after the anti-Fas injection and examined the hepatic injuries (Fig. 2(A)).

The mice that received injections of the control Ad.dE1.3 and anti-Fas antibody represented a remarkable increase in the serum ALT and AST levels, which were up to 2240±450 and 1665±391 IU/L (62 and 21 times as high as the normal levels), respectively, 24 h after the anti-Fas injection (Fig. 2(B) and (C)). The increases in the serum ALT and AST levels were significantly attenuated by an injection of either Ad.HB-EGF or Ad.HGF before the anti-Fas injection ($P<0.01$); the serum ALT and AST levels were similar (i.e. no statistically significant differences between these two groups) and less than 230 IU/L in both groups. On the other hand, the serum ALT and AST levels 36 h after the anti-Fas injection in the Ad.HB-EGF-treated mice were remarkably lower than those in not only the control Ad.dE1.3-treated but also the Ad.HGF-treated mice. The serum ALT and AST levels in the Ad.HB-EGF-treated mice were 12 and 8.4 times (at 24 h) and 2.0 and 3.1 times (at 36 h) as low as those in the control Ad.dE1.3-treated mice, respectively. Those in the Ad.HGF-treated mice were 10 and 8.1 times (at 24 h) and 0.7 and 0.9 times (i.e. no protective phenotype) (at 36 h), as low as those in the control Ad.dE1.3-treated ones, respectively. Thus, these results indicate that HB-EGF has a more potent inhibitory effect on Fas-induced liver injuries than HGF, at least for the present condition.

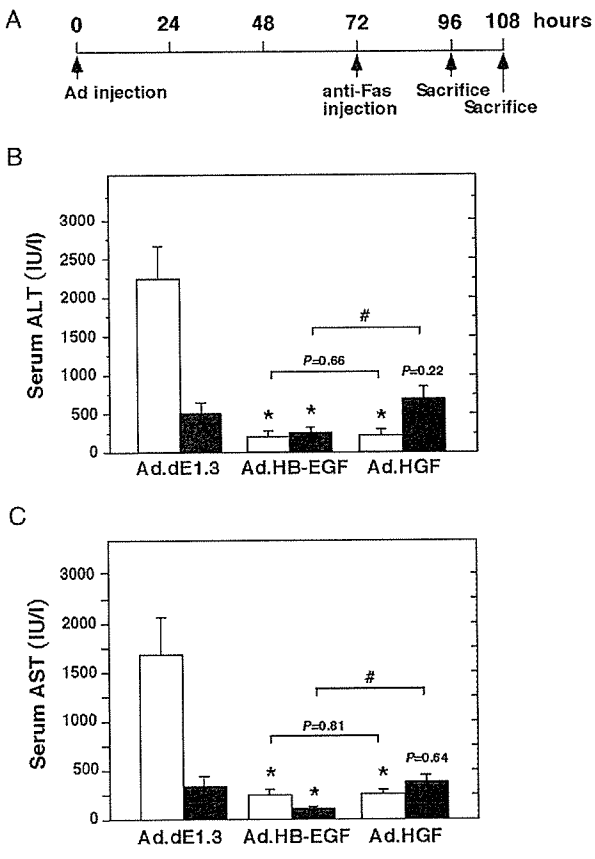

Fig. 2. Experimental schedule and liver enzymes after HB-EGF or HGF gene therapy for Fas-induced liver injury. (A) Experimental schedule of all the following therapeutic experiments. Mice ($n=10$, each group) received intraperitoneal injections of 4 μg of agonistic anti-Fas antibody 72 h after a tail vein injection of either Ad.hHB-EGF, Ad.hHGF or Ad.dE1.3 (1×10^{11} particles). The mice were then sacrificed, and liver and blood samples collected 24 or 36 h after injection of the anti-Fas antibody (i.e. 96 or 108 h after adenoviral injection). The serum ALT and AST levels at 24 (white bars) or 36 (black bars) hours after injection of the anti-Fas antibody are shown on (B) and (C), respectively (* $P<0.01$, either Ad.HB-EGF or Ad.HGF vs. control Ad.dE1.3: # $P<0.01$, Ad.HB-EGF vs. Ad.HGF).

3.3. Liver histopathology after HB-EGF or HGF gene therapy

The histological analysis of the livers at 24 and 36 h after the anti-Fas antibody injection in the control Ad.dE1.3-treated mice demonstrated severe liver injury with prominent apoptotic changes, as described previously [14,15] (Fig. 3). Briefly, apoptotic bodies characterized by nuclear and cell fragmentation within the shrunken and condensed cytoplasm were found, and there were a number of cells, consisting of spindle-shaped activated Kupffer cells, mononuclear cells and neutrophils, in the sinusoid. Such findings have often been observed in human patients with liver injuries as the apopto-necro-inflammatory reaction [33,36].

In contrast, there were minimal histopathological findings in the liver in the Ad.HB-EGF- or Ad.HGF-treated mice 24 and 36 h after the anti-Fas antibody injection; the inhibitory effect against liver injury as assessed by histopathologic observation on the H-E-stained slides in these mice was seemingly much more prominent than that assessed by the serum ALT and AST levels, as shown above. Apoptotic bodies were rarely seen, and the inflammatory reaction characterized by Kuppfer cell hyperplasia and accumulated inflammatory cells was not found. The difference in the histopathology of the liver between the Ad.HB-EGF- and Ad.HGF-treated mice was not clear at 24 h, but was remarkable at 36 h after the anti-Fas antibody injection. Notably, the pathological findings were still minimal in the Ad.HB-EGF-treated mice, but relatively prominent in the Ad.HGF-treated mice at 36 h after the anti-Fas antibody. These results indicated that HB-EGF has more potent cytoprotective and inhibitory effects against the Fas-induced apopto-necro-inflammatory reaction than HGF, at least for the present condition.

3.4. Potent anti-apoptotic effects of HB-EGF or HGF gene therapy

To obtain evidence that HB-EGF prevents hepatocyte apoptosis, apoptotic cells were detected by the in situ TUNEL assay (Fig. 4). In accordance with the

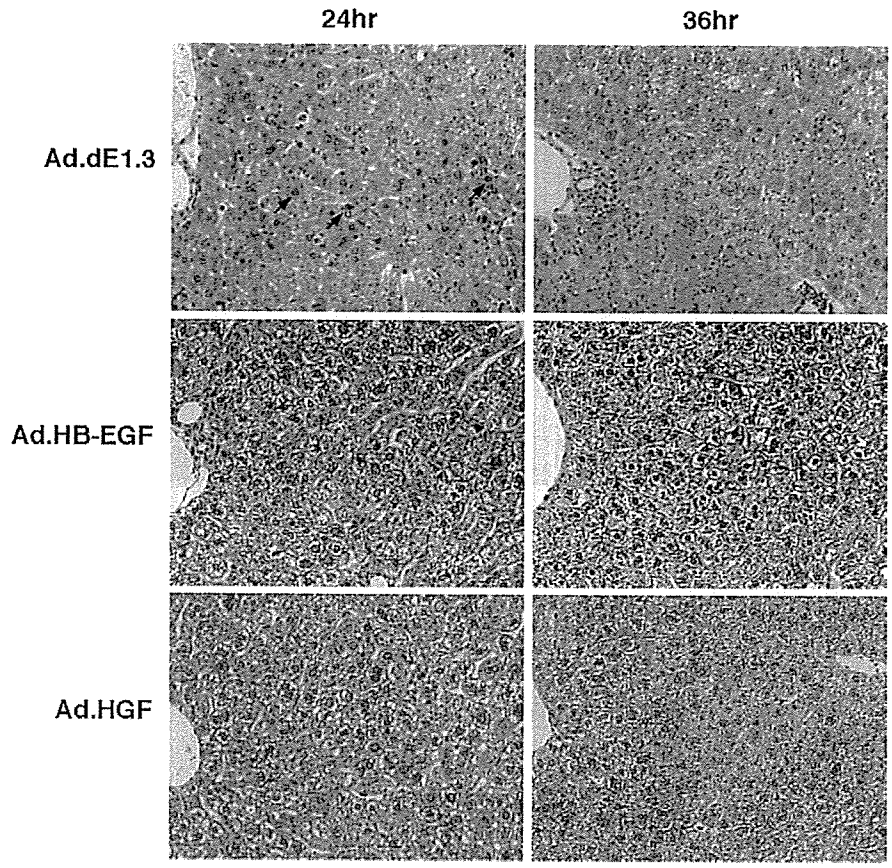

Fig. 3. Liver histopathology after HB-EGF or HGF gene therapy for Fas-induced liver injury. H-E stained liver slides of the mice that were given injections of the anti-Fas antibody and either Ad.dE1.3, Ad.HB-EGF or Ad.HGF on the protocol shown in Fig. 2(A) are shown. Arrows indicate typical acidophilic and apoptotic bodies. Original magnification, ×200. [This figure appears in colour on the web.]

histopathological findings on H-E slides, TUNEL-positive hepatocytes, approximately 10 or 6% of all hepatocytes, were observed throughout the liver parenchyma in the Ad.dE1.3-treated control mice 24 or 36 h after the anti-Fas antibody injection, respectively. Apoptotic bodies recognized in the disrupted hepatic cord or in the sinusoids were also TUNEL-positive. On the other hand, there were few (around 1%) TUNEL-positive hepatocytes in the liver of the mice treated with either Ad.HB-EGF or Ad.HGF at 24 and 36 h after the anti-Fas antibody injection. The morphometric and quantitative analysis of the TUNEL-positive cells revealed statistically significant differences between the control Ad.dE1.3- and either the Ad.HB-EGF- and Ad.HGF-treated groups ($P<0.01$), but no difference between the Ad.HB-EGF- and Ad.HGF-treated groups at 24 or 36 h after the anti-Fas antibody injection. These data suggest the anti-apoptotic effect of HB-EGF on hepatocytes is as potent as HGF.

3.5. HB-EGF induces liver regeneration more potently than HGF

We examined whether HB-EGF gene transduction and expression in the autocrine fashion may enhance liver regeneration after liver injury, and compared the degree of the inducible effect of HB-EGF to that of HGF by morphometric and quantitative analysis of Ki-67-positive cells (Fig. 5). In the control mice that received injections of Ad.dE1.3, Ki-67-positive replicating hepatocytes at 24 and 36 h after the anti-Fas antibody injection were 6.4 ± 0.7 and $12\pm2.2\%$, respectively, which were more than that of the intact liver without any treatment (less than 1%; data not shown). On the other hand, Ad.HGF injection significantly enhanced the hepatocyte replication at 24 and 36 h after the anti-Fas antibody up to 35.8 ± 2.8 and $28\pm3.0\%$, respectively ($P<0.01$, Ad.HGF vs. Ad.dE1.3). More promisingly, the Ad.HB-EGF injection induced the hepatocyte replication at 24 h after the anti-Fas antibody more efficiently up to $54.6\pm2.5\%$ ($P<0.01$, Ad.HB-EGF vs. Ad.HGF, and Ad.HB-EGF vs. Ad.dE1.3). The percentages of Ki-67-positive replicating hepatocytes in Ad.HB-EGF-treated mice at 36 h after the anti-Fas antibody were $29\pm2.9\%$, similar to those in the Ad.HGF-treated mice. Thus, HB-EGF gene transduction and expression in the hepatocytes induced the acute phase of liver regeneration after liver injury more potently than HGF.

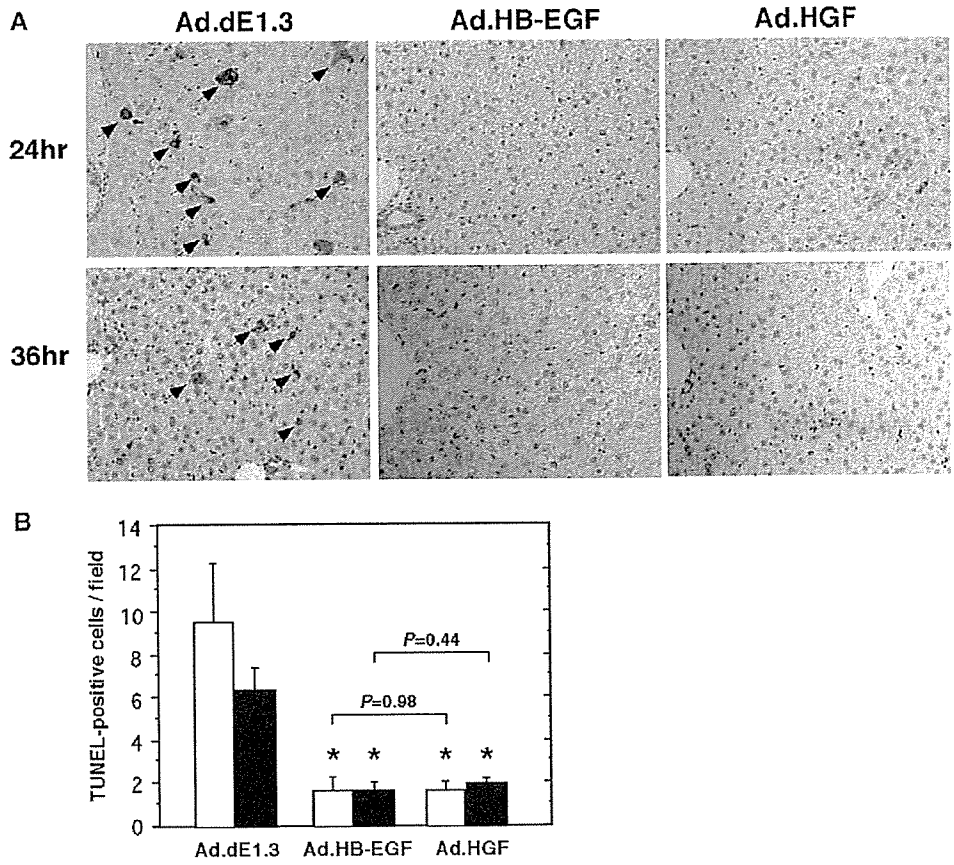

Fig. 4. TUNEL analysis of the liver after HB-EGF or HGF gene therapy for Fas-induced liver injury. (A) TUNEL staining using the liver tissue from the mice that were given injections of the anti-Fas antibody and either Ad.dE1.3, Ad.HB-EGF or Ad.HGF on the protocol shown in Fig. 2(A). Arrows indicate TUNEL-positive hepatocytes and apoptotic bodies. Original magnification, ×200. (B) The morphometric and quantitative analysis of TUNEL-positive cells at 24 (white bars) or 36 (black bars) hours after injection of the anti-Fas antibody in each group (* $P<0.01$, either Ad.HB-EGF or Ad.HGF vs. control Ad.dE1.3: # $P<0.01$, Ad.HB-EGF vs. Ad.HGF).

4. Discussion

It has been shown that exogenous HGF can be a potent therapeutic agent for liver disorders in terms of its beneficial effects of inhibiting liver injury and inducing liver regeneration, regardless of administration of the recombinant protein or the gene therapy strategy used [3,9–16]. In contrast to such extensive studies on HGF, the therapeutic potential of HB-EGF has not yet been explored. A few studies have shown the in vivo mitogenic effect of exogenous HB-EGF [26,27,37], but neither the anti-apoptotic effect on hepatocytes nor the inhibitory effect against liver injury have yet been studied. Thus, the present study revealed, for the first time, that HB-EGF might be a therapeutic agent for liver disorders in terms of both its anti-apoptotic and mitogenic effects on hepatocytes. On the other hand, we recently showed that in vivo HB-EGF gene transduction for myocardial infarction in the heart did not demonstrate therapeutic effects but instead exacerbated the remodeling, although HB-EGF is one of the essential cardiogenic and cardiotrophic factors [28]. Thus, the present results, taken together with our recent ones, are useful for understanding the physiological and pathological roles of HB-EGF. The phenotypic difference of HB-EGF may, at least in part, be due to potent and no cytoprotective effects of HB-EGF for hepatocytes and cardiomyocytes, respectively, although future extensive studies are necessary for overall elucidation.

Moreover, we obtained a further promising result in this study that the in vivo mitogenic and protective effects of HB-EGF on hepatocytes were more potent than those of HGF, at least in part and for the present condition. There are several possibilities why. The first possibility is the definitive difference between the HGF- and HB-EGF-dependent signal transduction pathways in hepatocytes related to the mitogenic phenotype; this is likely because their receptors, i.e. the c-met/HGF receptor and several EGF/erbB receptors, are different [3,20]. The second possibility is that this difference may result from the fact that HB-EGF plays more important roles in the early phase of liver regeneration than HGF. It was reported that the increase in the HB-EGF mRNA level occurred earlier than that of the HGF mRNA level during liver regeneration after partial hepatectomy or liver injury by hepatotoxins

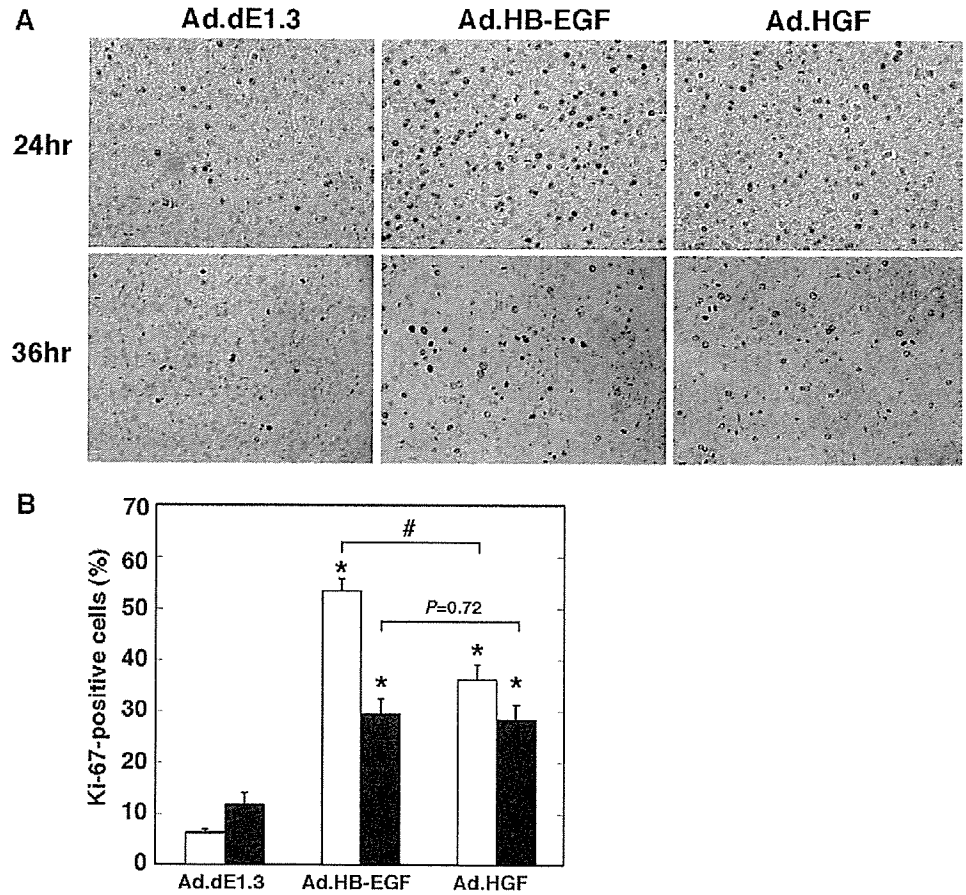

Fig. 5. Ki-67 immunohistochemistry of the liver after HB-EGF or HGF gene therapy for Fas-induced liver injury. (A) Immunohistochemistry against Ki-67 using the liver tissue from the mice that were given injections of the anti-Fas antibody and either Ad.dE1.3, Ad.HB-EGF or Ad.HGF on the protocol shown in Fig. 2(A). Original magnification, ×200. (B) The morphometric and quantitative analysis of Ki-67-positive cells at 24 (white bars) or 36 (black bars) hours after injection of the anti-Fas antibody in each group (* $P<0.01$, either Ad.HB-EGF or Ad.HGF vs. control Ad.dE1.3: # $P<0.01$, Ad.HB-EGF vs. Ad.HGF).

[24,25,38]. Another study showed that the additions of exogenous HB-EGF to nonparenchymal cells in the in vitro primary culture increased the HGF mRNA expressions in these cells, suggesting that HB-EGF may induce HGF production [24,26]. Thus, one hypothesis is that exogenous HB-EGF produced from the transduced human HB-EGF gene may sequentially activate several downstream factors, including HGF, and that these secondary effects together with the direct effect of HB-EGF may additively induce the higher mitogenic activity [39]. It would be interesting to investigate the detailed molecular mechanisms and the possibility of HB-EGF-induced liver regeneration in the case of a no priming event and the possible synergic or additive effects of HB-EGF and HGF combination gene therapy in future extensive studies.

In this study, we used an adenoviral vector and Fas-induced liver injury model solely for exploring the possibility and potential of HB-EGF gene therapy for liver diseases. A biologically important fact concerning the availability of hepatic HB-EGF gene therapy is that synthetic and proteolytic processes were reproduced even in hepatocytes, and that exogenous HB-EGF can efficiently activate hepatocytes in an artificial autocrine fashion. From the clinical viewpoint, more potent protective and mitogenic effects of HB-EGF for hepatocytes than those of HGF are apparently promising and potentially beneficial for treating liver disorders. However, it remains to be elucidated whether HB-EGF is a more clinically useful therapeutic agent for liver diseases than HGF. In actuality, some reports showed that HB-EGF was highly expressed in hepatocytes during hepatocarcinogenesis [40–42], and our recent study has shown that HB-EGF plays pathological roles in heart disorders [28]. In this regard, future studies are needed to investigate the clinical usefulness, including the possible adverse effects (e.g. fibrosis and hepatocarcinogenesis), of HB-EGF gene therapy for chronic hepatitis and liver cirrhosis, as we have carefully done in HGF gene therapy [29].

In conclusion, HB-EGF may have more potent protective and mitogenic activities for hepatocytes than HGF, at least

in part and for the present condition. In vivo HB-EGF gene transduction in the liver is therapeutic for Fas-induced liver injury.

Acknowledgements

This study was supported in part by a Grant-in-Aid for Scientific Research (C) from the Ministry of Education, Culture, Sports, Science and Technology of Japan, and in part by the Suzuken Memorial Foundation. We would like to thank Hatsue Oshika for her technical assistance, and Dr E. Mekada for providing the human HB-EGF cDNA.

References

[1] Michalopoulos GK. Liver regeneration: molecular mechanisms of growth control. Faseb J 1990;4:176–187.
[2] Fausto N, Laird AD, Webber EM. Liver regeneration. 2. Role of growth factors and cytokines in hepatic regeneration. Faseb J 1995;9: 1527–1536.
[3] Matsumoto K, Nakamura T. Hepatocyte growth factor (HGF) as a tissue organizer for organogenesis and regeneration. Biochem Biophys Res Commun 1997;239:639–644.
[4] Roberts RA, James NH, Cosulich SC. The role of protein kinase B and mitogen-activated protein kinase in epidermal growth factor and tumor necrosis factor alpha-mediated rat hepatocyte survival and apoptosis. Hepatology 2000;31:420–427.
[5] Webber EM, FitzGerald MJ, Brown PI, Bartlett MH, Fausto N. Transforming growth factor-alpha expression during liver regeneration after partial hepatectomy and toxic injury, and potential interactions between transforming growth factor-alpha and hepatocyte growth factor. Hepatology 1993;18:1422–1431.
[6] Birchmeier C, Gherardi E. Developmental roles of HGF/SF and its receptor, the c-Met tyrosine kinase. Trends Cell Biol 1998;8:404–410.
[7] Fausto N. Liver regeneration. J Hepatol 2000;32:19–31.
[8] Pistoi S, Morello D. Liver regeneration 7. Prometheus' myth revisited: transgenic mice as a powerful tool to study liver regeneration. Fed Am Soc Exp Biol J 1996;10:819–828.
[9] Ishiki Y, Ohnishi H, Muto Y, Matsumoto K, Nakamura T. Direct evidence that hepatocyte growth factor is a hepatotrophic factor for liver regeneration and has a potent antihepatitis effect in vivo. Hepatology 1992;16:1227–1235.
[10] Matsuda Y, Matsumoto K, Ichida T, Nakamura T. Hepatocyte growth factor suppresses the onset of liver cirrhosis and abrogates lethal hepatic dysfunction in rats. J Biochem Tokyo 1995;118:643–649.
[11] Ueki T, Kaneda Y, Tsutsui H, Nakanishi K, Sawa Y, Morishita R, et al. Hepatocyte growth factor gene therapy of liver cirrhosis in rats. Nat Med 1999;5:226–230.
[12] Hwang TH, Yoon BC, Jeong JS, Seo SY, Lee HJ. A single administration of adenoviral-mediated HGF cDNA permits survival of mice from acute hepatic failure. Life Sci 2003;72:851–861.
[13] Kosai KI, Finegold MJ, Thi-Huynh BT, Tewson M, Ou CN, Bowles N, et al. Retrovirus-mediated in vivo gene transfer in the replicating liver using recombinant hepatocyte growth factor without liver injury or partial hepatectomy. Hum Gene Ther 1998;9: 1293–1301.
[14] Kosai K, Matsumoto K, Nagata S, Tsujimoto Y, Nakamura T. Abrogation of Fas-induced fulminant hepatic failure in mice by hepatocyte growth factor. Biochem Biophys Res Commun 1998;244: 683–690.
[15] Kosai K, Matsumoto K, Funakoshi H, Nakamura T. Hepatocyte growth factor prevents endotoxin-induced lethal hepatic failure in mice. Hepatology 1999;30:151–159.
[16] Phaneuf D, Chen SJ, Wilson JM. Intravenous injection of an adenovirus encoding hepatocyte growth factor results in liver growth and has a protective effect against apoptosis. Mol Med 2000;6: 96–103.
[17] Higashiyama S, Abraham JA, Miller J, Fiddes JC, Klagsbrun M. A heparin-binding growth factor secreted by macrophage-like cells that is related to EGF. Science 1991;251:936–939.
[18] Raab G, Klagsbrun M. Heparin-binding EGF-like growth factor. Biochim Biophys Acta 1997;1333:F179–F199.
[19] Prenzel N, Zwick E, Daub H, Leserer M, Abraham R, Wallasch C, et al. EGF receptor transactivation by G-protein-coupled receptors requires metalloproteinase cleavage of proHB-EGF. Nature 1999;402: 884–888.
[20] Iwamoto R, Mekada E. Heparin-binding EGF-like growth factor: a juxtacrine growth factor. Cytokine Growth Factor Rev 2000;11: 335–344.
[21] Goishi K, Higashiyama S, Klagsbrun M, Nakano N, Umata T, Ishikawa M, et al. Phorbol ester induces the rapid processing of cell surface heparin-binding EGF-like growth factor: conversion from juxtacrine to paracrine growth factor activity. Mol Biol Cell 1995;6: 967–980.
[22] Ito N, Kawata S, Tamura S, Kiso S, Tsushima H, Damm D, et al. Heparin-binding EGF-like growth factor is a potent mitogen for rat hepatocytes. Biochem Biophys Res Commun 1994;198:25–31.
[23] Higashiyama S, Abraham JA, Klagsbrun M. Heparin-binding EGF-like growth factor stimulation of smooth muscle cell migration: dependence on interactions with cell surface heparan sulfate. J Cell Biol 1993;122:933–940.
[24] Kiso S, Kawata S, Tamura S, Higashiyama S, Ito N, Tsushima H, et al. Role of heparin-binding epidermal growth factor-like growth factor as a hepatotrophic factor in rat liver regeneration after partial hepatectomy. Hepatology 1995;22:1584–1590.
[25] Kiso S, Kawata S, Tamura S, Ito N, Tsushima H, Yamada A, et al. Expression of heparin-binding EGF-like growth factor in rat liver injured by carbon tetrachloride or D-galactosamine. Biochem Biophys Res Commun 1996;220:285–288.
[26] Kiso S, Kawata S, Tamura S, Umeki S, Ito N, Tsushima H, et al. Effects of exogenous human heparin-binding epidermal growth factor-like growth factor on DNA synthesis of hepatocytes in normal mouse liver. Biochem Biophys Res Commun 1999;259:683–687.
[27] Kiso S, Kawata S, Tamura S, Inui Y, Yoshida Y, Sawai Y, et al. Liver regeneration in heparin-binding EGF-like growth factor transgenic mice after partial hepatectomy. Gastroenterology 2003;124:701–707.
[28] Ushikoshi H, Takahashi T, Chen X, Khai NC, Esaki M, Goto K, et al. Local overexpression of HB-EGF exacerbates remodeling following myocardial infarction by activating noncardiomyocytes. Lab Invest 2005;85:862–873.
[29] Yuge K, Takahashi T, Nagano S, Terazaki Y, Murofushi Y, Ushikoshi H, et al. Adenoviral gene transduction of hepatocyte growth factor elicits inhibitory effects for hepatoma. Int J Oncol 2005; 27:77–85.
[30] Chen SH, Chen XH, Wang Y, Kosai K, Finegold MJ, Rich SS, et al. Combination gene therapy for liver metastasis of colon carcinoma in vivo. Proc Natl Acad Sci USA 1995;92:2577–2581.
[31] Terazaki Y, Yano S, Yuge K, Nagano S, Fukunaga M, Guo ZS, et al. An optimal therapeutic expression level is crucial for suicide gene therapy for hepatic metastatic cancer in mice. Hepatology 2003;37: 155–163.
[32] Peeters MJ, Patijn GA, Lieber A, Meuse L, Kay MA. Adenovirus-mediated hepatic gene transfer in mice: comparison of intravascular and biliary administration. Hum Gene Ther 1996;7: 1693–1699.

[33] Oksuz M, Akkiz H, Isiksal YF, Saydaogluc G, Serin M, Kayaselcuk F, et al. Expression of Fas antigen in liver tissue of patients with chronic hepatitis B and C. Eur J Gastroenterol Hepatol 2004;16:341–345.
[34] Kondo T, Suda T, Fukuyama H, Adachi M, Nagata S. Essential roles of the Fas ligand in the development of hepatitis. Nat Med 1997;3: 409–413.
[35] Ogasawara J, Watanabe-Fukunaga R, Adachi M, Matsuzawa A, Kasugai T, Kitamura Y, et al. Lethal effect of the anti-Fas antibody in mice. Nature 1993;364:806–809.
[36] Ferrell L. Liver pathology: cirrhosis, hepatitis, and primary liver tumors. Update and diagnostic problems. Mod Pathol 2000;13: 679–704.
[37] Mitchell C, Nivison M, Jackson LF, Fox R, Lee DC, Campbell JS, et al. Heparin-binding epidermal growth factor-like growth factor links hepatocyte priming with cell cycle progression during liver regeneration. J Biol Chem 2005;280:2562–2568.
[38] Kinoshita T, Tashiro K, Nakamura T. Marked increase of HGF mRNA in non-parenchymal liver cells of rats treated with hepatotoxins. Biochem Biophys Res Commun 1989;165:1229–1234.
[39] Scheving LA, Stevenson MC, Taylormoore JM, Traxler P, Russell WE. Integral role of the EGF receptor in HGF-mediated hepatocyte proliferation. Biochem Biophys Res Commun 2002;290:197–203.
[40] Inui Y, Higashiyama S, Kawata S, Tamura S, Miyagawa J, Taniguchi N, et al. Expression of heparin-binding epidermal growth factor in human hepatocellular carcinoma. Gastroenterology 1994; 107:1799–1804.
[41] Miyoshi E, Higashiyama S, Nakagawa T, Suzuki K, Horimoto M, Hayashi N, et al. High expression of heparin-binding EGF-like growth factor in rat hepatocarcinogenesis. Int J Cancer 1996;68:215–218.
[42] Kiso S, Kawata S, Tamura S, Miyagawa J, Ito N, Tsushima H, et al. Expression of heparin-binding epidermal growth factor-like growth factor in the hepatocytes of fibrotic rat liver during hepatocarcinogenesis. J Gastroenterol Hepatol 1999;14:1203–1209.

ELSEVIER

Cardiovascular Research 69 (2006) 476 – 490

Cardiovascular Research

www.elsevier.com/locate/cardiores

Bone marrow-derived myocyte-like cells and regulation of repair-related cytokines after bone marrow cell transplantation

Yu Misao [a], Genzou Takemura [a], Masazumi Arai [a], Shigeru Sato [c], Koji Suzuki [a], Shusaku Miyata [a], Ken-ichiro Kosai [b], Shinya Minatoguchi [a], Takako Fujiwara [d], Hisayoshi Fujiwara [a,*]

[a] *Department of Cardiology, Regeneration Medicine and Bioethics, Gifu University Graduate School of Medicine, 1-1 Yanagido, Gifu, 501-1194, Japan*
[b] *Gene Therapy and Regenerative Medicine, Gifu University Graduate School of Medicine, Gifu, Japan*
[c] *Central Institute for Electron Microscopic Research, Nippon Medical School, Tokyo, Japan*
[d] *Department of Food Science (T.F.), Kyoto Women's University, Kyoto, Japan*

Received 4 August 2005; received in revised form 19 October 2005; accepted 1 November 2005
Available online 20 December 2005
Time for primary review 27 days

Abstract

Objective: Whether bone marrow cells injected following acute myocardial infarction (MI) transdifferentiate into cardiomyocytes remains controversial, and how these cells affect repair-related cytokines is not known.
Methods: Autologous bone marrow-derived mononuclear cells (BM-MNCs) labeled with DiI, 1,1′-dioctadecyl-1 to 3,3,3′,3′-tetramethylindocarbocyanine perchlorate, or saline were intravenously injected into rabbits 5 h following a 30-min ischemia and reperfusion protocol, and cardiac function and the general pathology of the infarcted heart were followed up 1 and 3 months post-MI. To search for regenerated myocardium, electron microscopy as well as confocal microscopy were performed in the infarcted myocardium 7 days post-MI. Expression levels of repair-related cytokines were evaluated by immunohistochemistry and Western blotting.
Results: Improvements in cardiac function and reductions in infarct size were observed in the BM-MNC group 1 month and 3 months post-MI. Using electron microscopy 7 days after infarction, clusters of very immature (fetal) and relatively mature cardiomyocytes undergoing differentiation were identified in the infarcted anterior LV wall in the BM-MNC group, though their numbers were small. These cells contained many small and dense DiI particles (a BM-MNC marker), indicating that cardiomyocytes had regenerated from the injected BM-MNCs. The expression of both transforming growth factor-β, which stimulates collagen synthesis and matrix metalloproteinase-1, a collagenase, were both down-regulated 7 days and 1 month post-MI in the BM-MNC group. Stromal cell-derived factor-1, which is known to recruit BM-MNCs into target tissues, was overexpressed in the infarcted areas of BM-MNC hearts 7 days post-MI.
Conclusions: Intravenous transplantation of BM-MNCs leads to the development of BM-MNC-derived myocyte-like cells and regulates the expression of repair-related cytokines that facilitate repair following myocardial infarction.

Keywords: Myocardial regeneration; Ultrastructure; Cardiac repair; Bone marrow; Cytokines

1. Introduction

Transplantation of bone marrow-derived mononuclear cells (BM-MNCs), including hematopoietic and mesenchymal stem cells, following acute myocardial infarction (MI) diminishes left ventricular (LV) remodeling, improves LV function, and reduces the size of old infarcts in post-MI hearts [1–3]. Nevertheless, the presence of BM-derived cardiomyocytes in infarcted myocardium remains controversial because although they are readily detectable in some cases [1], they are undetectable in others [4–6]. Contributing to this discrepancy may be an overestimation or underestimation of the numbers of BM-derived cardiomyo-

* Corresponding author. Tel.: +81 58 230 6520; fax: +81 58 230 6521.
E-mail address: gifuim-gif@umin.ac.jp (H. Fujiwara).

0008-6363/$ - see front matter © 2005 European Society of Cardiology. Published by Elsevier B.V. All rights reserved.
doi:10.1016/j.cardiores.2005.11.001

cytes as a result of technical problems with the methods used. For instance, autofluorescence can interfere with the confocal microscopic analysis of immunofluorescence. In addition, earlier studies of post-MI regeneration were carried out using models that involved the permanent occlusion of coronary arteries, though clinical treatment for acute MI generally involves recanalization of infarct-related coronary arteries by thrombolysis or percutaneous angioplasty. Bearing these issues in mind, one of our aims in the present study was to use electron microscopy to determine whether intravenously injected autologous BM-MNCs can transdifferentiate into cardiomyocytes during post-MI repair in a rabbit ischemia–reperfusion model.

We also recently reported that the beneficial effects of granulocyte colony-stimulating factor are likely associated with the expression of repair-related cytokines as well as with cardiomyocyte regeneration [7], which suggests that BM-MNCs may also exert an effect on the expression of repair-related cytokines. Therefore, the second aim of this study was to determine whether expression levels of transforming growth factor (TGF)-β, a mediator stimulating collagen synthesis; matrix metalloproteinase (MMP)-1, a collagenase; or stromal cell-derived factor (SDF)-1, a chemoattractant known to recruit BM-MNCs into target tissues, correlate with post-MI repair after BM-MNC treatment.

2. Materials and methods

All the rabbits received humane care in accordance with the Guide for Care and Use of Laboratory Animals, published by the U.S. National Institutes of Health (NIH publication 8523, revised 1985). The study protocol was approved by the Ethics Committee of Gifu University School of Medicine, Gifu, Japan.

2.1. Autologous BM-MNCs

Male Japanese white rabbits weighing 1.9–2.5 kg were anesthetized by intravenous injection with 30 mg/kg of sodium pentobarbital. Approximately 10 ml of iliac BM was aspirated and suspended in 20 ml of RPMI-1640 medium (Sigma) containing 2000 U of heparin sodium. BM-MNCs were then isolated by centrifugation on a Ficoll gradient (JIMRO, Takasaki, Japan), and approximately 1.0×10^8 BM-MNCs were suspended in 2 ml of phosphate-buffered saline.

2.2. Ischemia–reperfusion infarct model and injection of BM-MNCs

One hour after the aspiration of BM, a 30-min ischemia and reperfusion protocol was carried out as previously described [7]. The rabbits were randomly assigned to either a BM-MNC or saline group, which were respectively administered the autologous BM-MNCs or 2 ml of saline via an ear vein after 5 h of reperfusion.

2.3. Protocol I: cardiac function and pathology

2.3.1. Echocardiography

The 90 rabbits in the BM-MNC and saline groups received trans-thoracic echocardiography (Aloka SSD4000) using a 7.5-mHz sector scan probe 7 days, 1 month and 3 months after the 30-min ischemia ($n=15$ in each group). LV anterior wall thickness (AWT, mm), posterior wall thickness (PWT, mm), body weight-corrected LV end-diastolic dimension (EDD/BW, mm/kg), and LV ejection fraction (EF, %) were measured. All measurements were made by two examiners (Y.M. and M.A.) blinded to the conditions.

2.3.2. General pathology

Following the echocardiography, each of the 90 rabbits was sacrificed with an overdose of pentobarbital after heparinization (500 U/kg), after which body weight and LV weight were measured. The LV was then fixed in 10% buffered formalin and sliced into 7 transverse sections parallel to the atrio-ventricular ring from the apex to the base. The slices were embedded in paraffin, cut to a thickness of 4 μm, and stained with hematoxylin and eosin (HE) and Sirius red. For transversely sliced preparations with infarction, the LV wall areas, infarcted areas, non-infarcted areas, and Sirius red-positive collagen areas were calculated using an image analyzer connected to a light microscope (LUZEX-F, NIRECO, Tokyo) and expressed as mm^2/slice/body weight (kg). Comparisons were made by two persons (Y.M. and M.A.) blinded to the conditions.

2.3.3. Immunohistochemistry

Using the indirect immunoperoxidase method, immunohistochemical staining was carried out with the following monoclonal antibodies (mAbs) that all cross-react with rabbit tissues: mouse anti-rabbit sarcomeric actin mAb (1:75; DAKO), mouse anti-human endothelial cell CD31 mAb (1:100; DAKO), mouse anti-human α-smooth muscle actin mAb (1:250; DAKO, 1A4), mouse anti-macrophage mAb (1:100; DAKO, RAM11), mouse anti-human MMP-1 mAb (1:500; Daiichi Fine Chemical, F-67), mouse anti-human TGF-β mAb (1:2000; Oxford Biotechnology.) and mouse anti-human/mouse SDF-1 mAb (1:120; R&D Systems). Morphometric analyses were carried out by two persons (Y.M. and G.T.) blinded to the conditions.

2.4. Protocol II: DiI-labeling of BM-MNCs, electron microscopy, laser scanning confocal microscopy and Western blotting

BM-MNCs were isolated from 12 rabbits as described above and then incubated for 30 min at 37 °C. To label the

cells with 1,1′-dioctadecyl-1 to 3,3,3′,3′-tetramethylindocarbocyanine perchlorate dye (DiI, Molecular Probes), 25 μl of a 2-mg/ml solution of DiI in dimethyl sulfoxide (Wako, Japan) was added to the BM-MNCs from 6 of the rabbits [8,9]. Thereafter, those 12 rabbits plus 6 in a saline group were subjected to the 30-min ischemia and reperfusion protocol, and after 5 h of reperfusion, the autologous BM-MNCs, with or without DiI, or 2 ml of saline (6 rabbits in each group) were injected via an ear vein. Seven days post-MI, the rabbits were sacrificed under anesthesia, and the hearts were immediately excised and placed in iced PBS (less than 4 °C) and cut transversely at the center of the infarcted anterior LV wall. The upper half was subsequently used for electron microscopy and laser-scanning confocal microscopy, and the lower half was used for Western blot analysis.

Immediately after sacrifice (within 1 min), myocardial tissue from the upper infarcted anterior LV wall (AW-MI) and non-infarcted posterior LV wall (PW-NMI) of each heart was cut into 1-mm cubes, fixed in 2.5% glutaraldehyde in 0.1 mol/L phosphate buffer (pH 7.4) at 4 °C for 4 h, and post-fixed in 1% buffered osmium tetroxide for 2 h. The samples were then dehydrated through a graded ethanol series and embedded in epoxy resin. One serial thin section (80 nm) was conventionally double-stained with uranylacetate for 10 min and lead citrate for 4 min and used for an electron microscopic (H-800, Hitachi) detection of ultrastructure. Another thin section stained with lead citrate for 1 min was used for the detection of DiI particles at magnifications greater than 20,000×.

In addition, other tissue samples obtained from the upper AW-MI and PW-NMI (three samples each, approximately 3 × 3 × 2 mm) were embedded in OCT compound (Miles Scientific), snap-frozen in liquid nitrogen and cut into 6-μm-thick sections using a cryostat for immunohistochemical analysis. Immunofluorescence microscopy was carried out using mouse anti-troponin I mAb (1:5000; CHEMICON), mouse anti-human endothelial cell CD31 mAb, and mouse anti-human α-smooth muscle actin mAb. Nuclei were stained with Hoechst 33342. The tissues were observed using a laser-scanning confocal microscope (LSM510 NLO, ZEISS, Tokyo), which enabled simultaneous analysis of the relationship between three different fluorescence and phase contrast images. Morphometric analyses were performed by two persons (Y.M. and M.A.) blinded to the conditions.

For Western blot analysis, tissues (approximately 200 mg) obtained from the center of the lower AW-MI and PW-NMI were snap-frozen in liquid nitrogen immediately after sacrifice. For the measurement of MMP-1, TGF-β and SDF-1, 50 mg of frozen tissue obtained from the hearts of sham, saline and BM-MNC-treated rabbits were homogenized in lysis buffer and centrifuged for 10 min at 10,000×*g* and 4 °C. MMP-1, TGF-β and SDF-1 were measured by Western blot analysis using the same Abs described for Protocol I. Signals were quantified by densitometry.

2.5. Protocol III: in vitro study

BM-MNCs and cultured adult cardiomyocytes [10] were left untreated or pretreated with DiI for 30 min at 37 °C, after which they were incubated for 7 days at 37 °C and processed for electron microscopy (fixed in 2.5% glutaraldehyde in 0.1 mol/L phosphate buffer [pH 7.4] for 30 min, post-fixed in 1% buffered osmium tetroxide for 1 h, dehydrated through graded ethanol and embedded in epoxy resin).

2.6. Statistical analysis

All values are presented as means±S.D. Differences between the saline and BM-MNC groups were assessed by two-way repeated-measures analysis of variance (ANOVA), followed with a post hoc Tukey–Kramer's test. Linear regression techniques were used to evaluate the correlation between pathological/echocardiographic parameters and the expression of cytokines. Values of $p<0.05$ were considered significant.

3. Results

3.1. Mortality

All rabbits in the saline and BM-MNC groups survived until sacrificed 7 days, 1 month or 3 months post-MI.

3.2. Echocardiography

LV anterior wall thickness 1 and 3 months after MI was significantly greater in the BM-MNC group (2.2±0.2 and 2.3±0.2 mm, respectively) than the saline group (1.6±0.2 and 1.8±0.2 mm, respectively), but there was no significant difference in posterior wall thickness between the two groups at any time point as shown in Fig. 1a and b. In the saline group, additionally, EFs were significantly lower and EDD/BWs were significantly higher 1 month and 3 months post-MI than before infarction (Fig. 1c and d). These adverse effects were significantly attenuated in the BM-MNC group, indicating an improved LV function and reduced remodeling (Fig. 1c and d).

3.3. General histology

Seven days post-MI, the infarcted areas showed mostly granulation with numerous myofibroblasts and small vessels in both the saline and BM-MNC groups. In addition, residual necrotic areas were observed in the centers of the granulated tissues. The numbers of small arteries positive for α-smooth muscle actin (a specific marker of smooth muscle cells) and microvessels positive for CD31 (a specific endothelial marker) were significantly larger in the BM-MNC group than the saline group (Fig. 2a and b), as were numbers of macrophages positive for RAM 11 (a specific

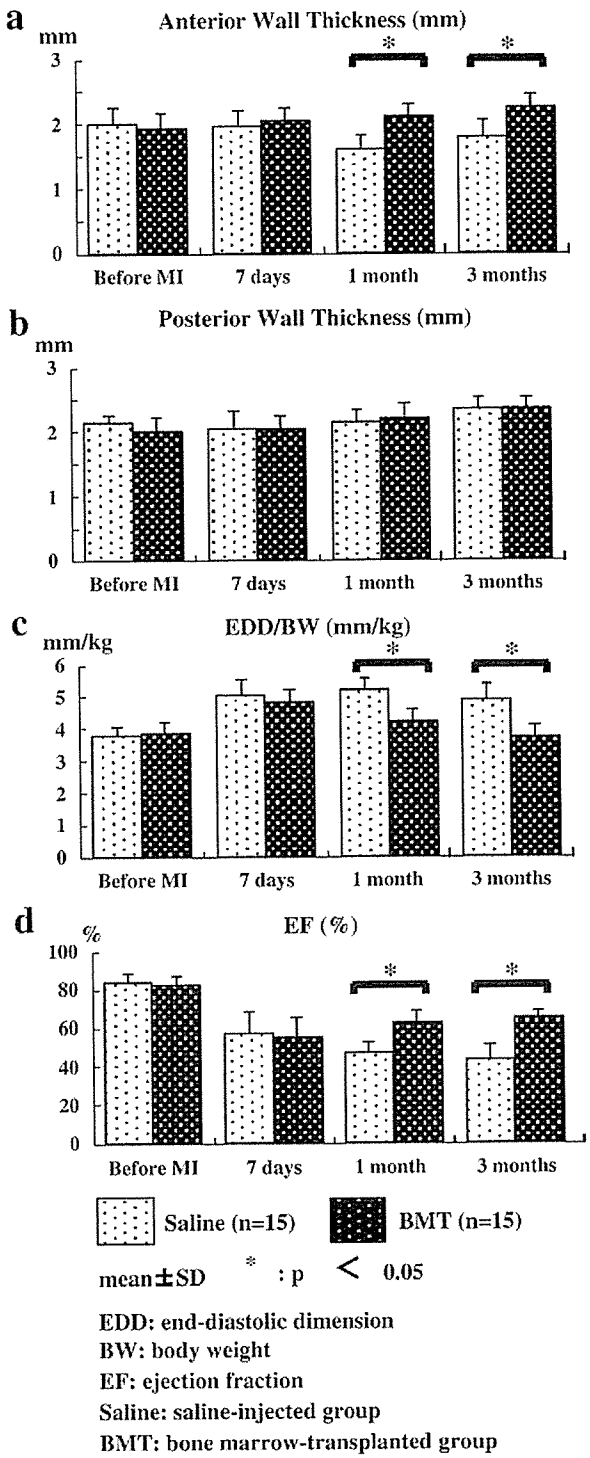

Fig. 1. BM-MNC treatment improves echocardiographic findings. AWTs, PWTs, EFs and EDD/BW ratios obtained 7 days, 1 month and 3 months post-MI.

marker of macrophages) and multinuclear giant cells (Fig. 2c). On the other hand, the respective transverse diameters of the cardiomyocytes in the AW-MI and PW-NMI were similar in the saline and BM-MNC groups, though the size of the cells was significantly greater in the AW-MI than the PW-NMI in each group (Fig. 3a).

One and three months post-MI, LV weight and LV wall area were also similar between the BM-MNC and saline groups (Fig. 3b and c), and the infarcted areas showed scar tissue comprised of collagen and fatty tissue in both the saline and BM-MNC groups. When the LV walls were stained with HE and the collagen with Sirius red, however, the old infarcts were found to be significantly smaller in the BM-MNC group than in the saline group (Fig. 3d and e). Conversely, the non-infarcted areas were significantly larger in the BM-MNC group (Fig. 3f). In both groups, the numbers of CD31-positive capillaries, α-smooth muscle actin-positive small arteries, and RAM 11-positive macrophages were markedly smaller than the numbers seen 7 days after infarction and were similar (Fig. 2a–c).

3.4. Electron microscopy

An extensive search using electron microscopy revealed unfamiliar mononuclear cells in the AW-MI of BM-MNC hearts 7 days post-MI. Differing from normal adult cardiomyocytes with mature sarcomeres (Fig. 4a), these cells were relatively large and electron-lucent, and their cytoplasm lacked cross-striations, but was loosely or tightly packed with myofilaments, the size of which suggested they were thin filaments (Fig. 4b1). Although reminiscent of myofibroblasts or smooth muscle cells, these cells had several features that were specific to immature cardiomyocytes: first, they were connected to one another by intercalated discs, a specific structure of striated muscle cells, including cardiomyocytes, and the intercalated discs contained distinct desmosomes and gap junctions (Fig. 4b2, c2, e and f). In intercalated discs, we did not detect clear fascia adherence; the absence is probably due to not-well-developed myofilaments in the cytoplasm; and second, Z disc-like structures were scattered among the myofilaments (Fig. 4c, c1 and d). There were small structures that appeared like myofilaments tied up into bundles in the vicinity of intermingling thick filaments, a configuration similar to the developing Z discs observed in fetal hearts [11]. Other, apparently more differentiated, cell types were also found, which contained better developed, but still not complete, Z discs (Fig. 4f). Such cells formed occasional clusters (Fig. 4b and c). Taken together, these findings suggest the presence of myocyte-like cells undergoing differentiation in the AW-MI of BM-MNC hearts, though their numbers were small: on average, the number of observed myocyte-like cells was 4.6±3.9/heart in the BM-MNC group and 0±0/heart in the saline group.

To determine whether these myocyte-like cells were derived from bone marrow cells, we first examined cultured BM-MNCs and isolated adult cardiomyocytes that had been incubated with DiI. We detected no DiI in specimens conventionally double-stained with uranyl acetate and lead citrate for electron microscopic examination (Fig. 5a).

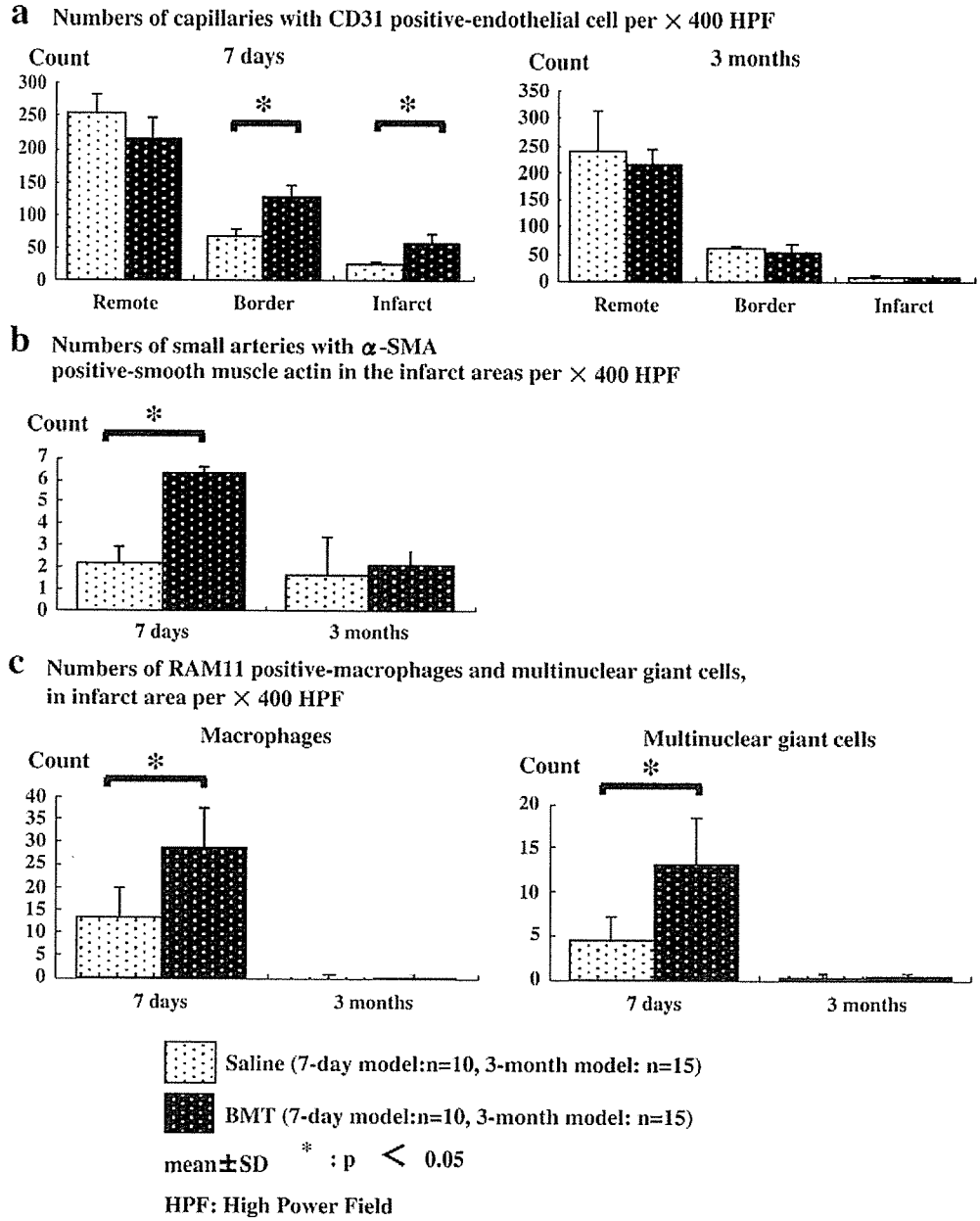

Fig. 2. Interstitial cell densities. The numbers of CD31-positive capillaries, α-smooth muscle actin-positive small arteries, RAM 11-positive macrophages and giant cells observed 7 days post-MI. Cells were counted in each of 15 serial fields per rabbit under a light microscopy. The border zone was defined as surviving myocardial tissue areas within 1 mm of infarcted areas.

However, when specimens were stained for only a short time with lead citrate alone, DiI was detected as 5-nm particles that accumulated within the cells and were scattered in the cytoplasm, mitochondria and lysosomes (Fig. 5b–d). These particles were not observed in cells that were not incubated with DiI. When DiI-labeled BM-MNC and control hearts were examined using the same method, DiI particles were detected in a total of 20 myocyte-like cells in the BM-MNC hearts (Fig. 5e–f) and were also occasionally found in pericytes present in the infarcted area (Fig. 5g and h). In addition, there was no evidence of DiI particles in BM-MNC and saline hearts not labeled with DiI.

3.5. Confocal microscopy

Within tissue sections obtained from the AW-MI of DiI-labeled BM-MNC hearts 7 days after MI, 0.14±0.13% of troponin I-positive (green) cells were also DiI-positive (red), and these cells formed a cluster (Fig. 6b). In addition, 0.05±0.04% of the cells positive for α-smooth muscle actin

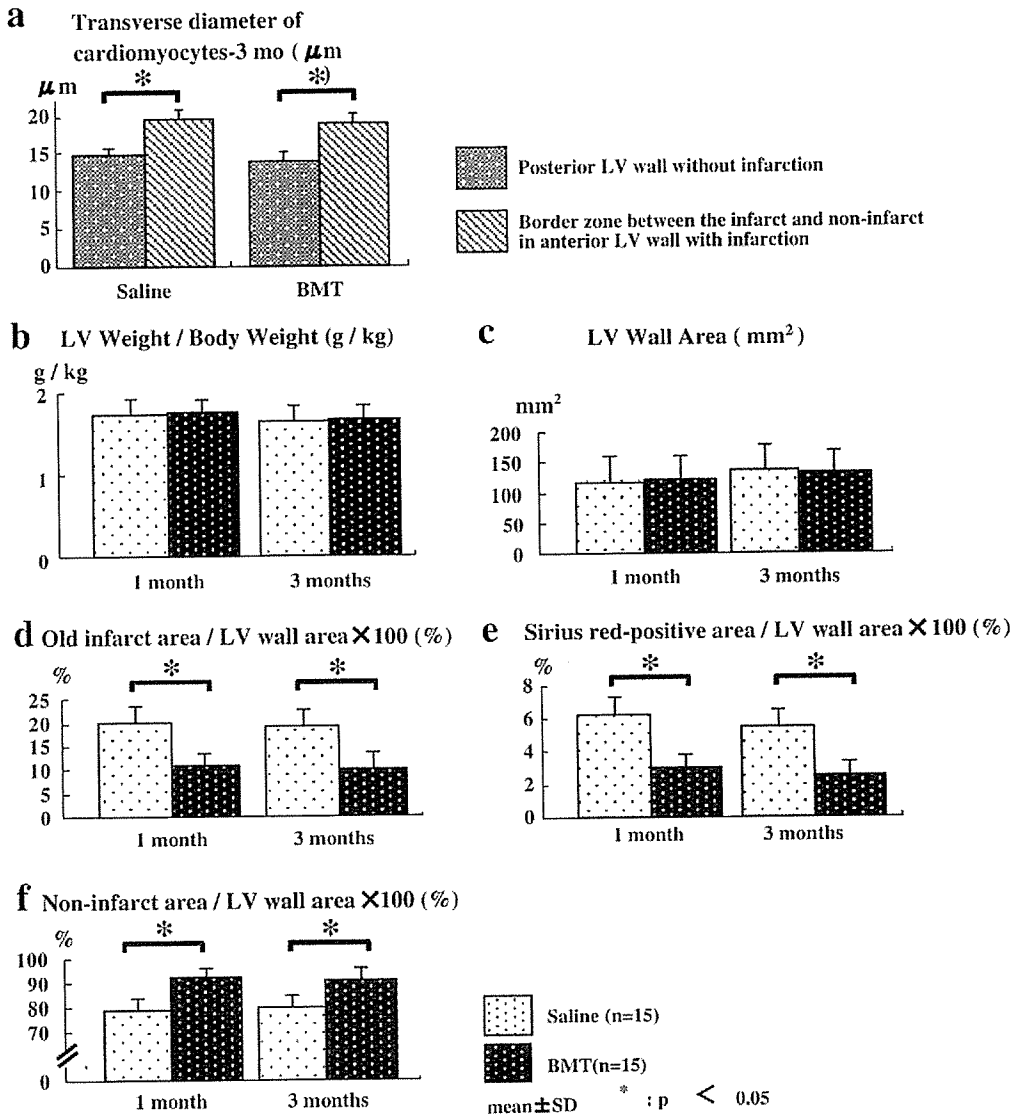

Fig. 3. BM-MNC treatment reduces infarct size and increases non-infarcted area. Shown are LV weight, LV wall area, cardiomyocyte size, non-infarcted area and old infarct areas. The border zone was defined as in the legend to Fig. 2.

and 0.3±0.3% of cells positive for CD31 were also positive for DiI.

3.6. TGF-β, MMP-1 and SDF-1

Immunohistochemical analysis showed TGF-β to be expressed in endothelial cells, smooth muscle cells and myofibroblasts (Fig. 7 and Supplementary data 1). In the saline groups, the level of expression within the infarcted areas was highest 7 days and 1 month post-MI (2.2±0.3 and 2.4±0.3, respectively) but had declined by 3 months (1.6±0.8) (Fig. 8a). There was significantly less expression of TGF-β in the infarcted areas of BM-MNC hearts 7 days and 1 month post-infarction (1.1±0.4 and 1.2±0.8, respectively), but by 3 months, the level of expression in the BM-MNC group (1.4±0.7) was similar to that in the saline group (1.6±0.8).

MMP-1 was expressed in cardiomyocytes located at the border between the infarcted area and salvaged myocardial tissues (Fig. 7). In the saline group, the level of MMP-1 expression was highest 7 days and 1 month post-MI (2.6±0.4 and 2.4±0.6, respectively), but dropped significantly by 3 months (1.4±0.8) (Fig. 8b). As was seen with TGF-β, there was significantly less expression of MMP-1 in the BM-MNC group 7 days and 1 month post-MI (1.1±0.5 and 1.3±0.8, respectively).

Expression of SDF-1 was observed in endothelial cells, vascular smooth muscle cells, myofibroblasts and interstitial fibrous tissues within the infarcts 7 days post-MI. (Fig. 7 and Supplementary data 1) The level of SDF-1

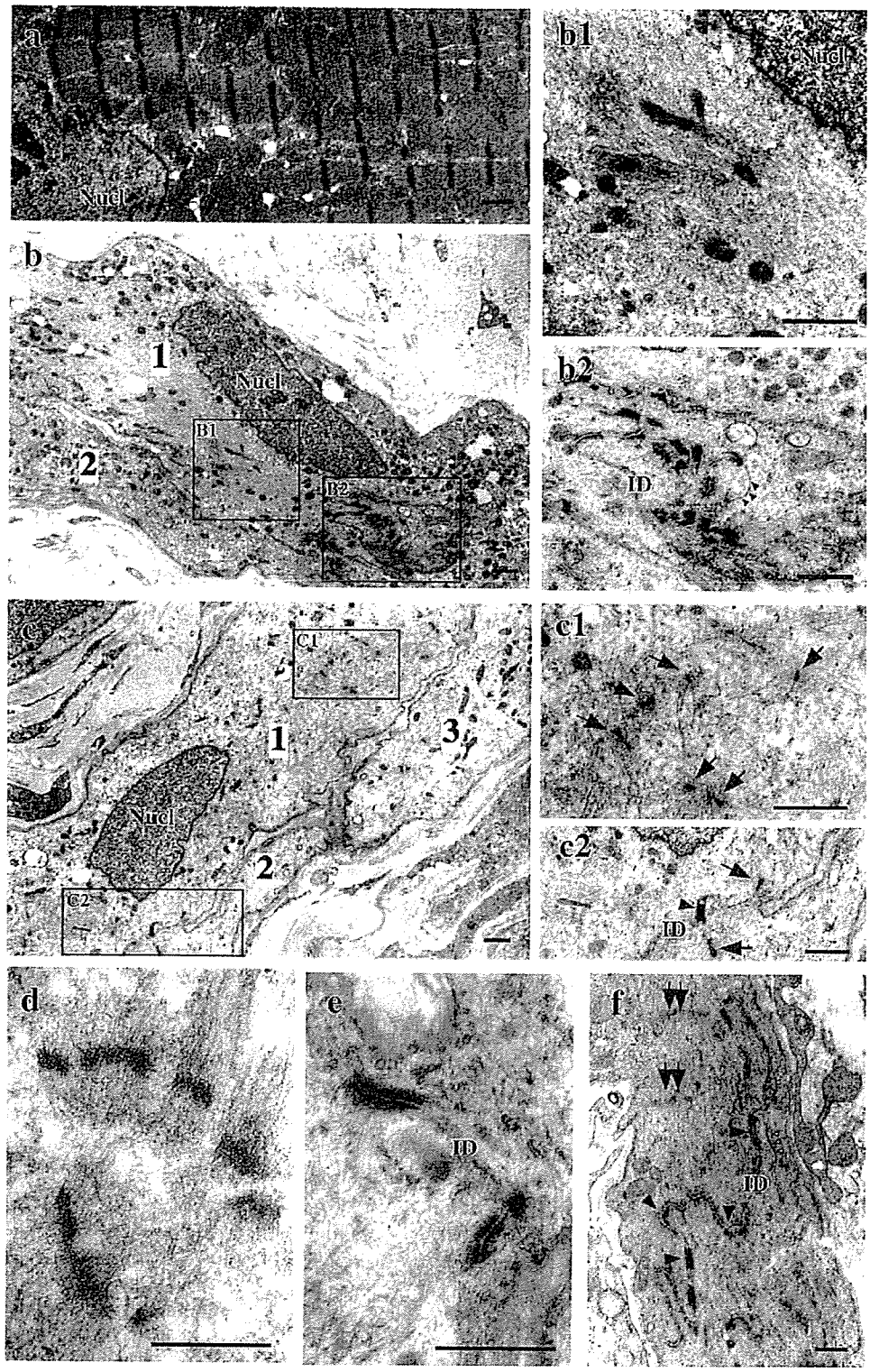

Fig. 4. Ultrastructure of myocyte-like cells in the infarcted anterior LV wall of the BM-MNC group 7 days post-MI. (a) Normal adult cardiomyocyte showing characteristic striations and mature sarcomeres. (b) Relatively large and electron-lucent immature cells; (b1 and b2) highly magnified images of the boxed portions in panel (b). Note the thin filaments filling the cytoplasm (b1), and that the cells were perpendicularly connected to one another by well-developed intercalated discs (ID) (b2). Small triple arrowheads indicate gap junctions (b2). (c) Z disk-like structures in myocyte-like cells. (c1 and c2) Highly magnified photographs of the boxed portions of panel (c); the cells contain Z disc-like structures (arrows) scattered in the cytoplasm (c1). An arrowhead indicates desmosome-containing intercalated discs (c2). (d and e) Myocyte-like cells; High magnification of Z disc-like structures (d) and desmosomes within an intercalated disc (e). (f) More developed Z discs (double arrows) connected to one another by intercalated discs (ID). Black and white arrowheads indicate, respectively, desmosomes and gap junction in ID.

expression was significantly higher in the BM-MNC group (2.6±0.3) than in the saline group (0.8±0.3) (Fig. 8c). No expression was detected in either group 1 and 3 months post-MI.

As shown in Fig. 9, Western blot analysis 7 days post-MI showed that the enhanced expression of TGF-β in the LV anterior wall with infarction and the LV posterior wall in the saline group was significantly down-regulated in the BM-MNC group. Pro-MMP-1 expression was enhanced in the LV anterior wall of the saline group and the enhancement was significantly inhibited in the BM-MNC group. The enhanced expression of SDF-1 in the LV anterior wall 24 h after MI disappeared 7 days later in the saline group. In the BM-MNC group, however, SDF-1 was markedly expressed in both the LV anterior and posterior walls 7 days post-MI.

3.7. Correlation between cytokine expression, LV function and remodeling, and old infarct size

One month after infarction, levels of TGF-β and MMP-1 were negatively and significantly correlated with AWT/PWT ratios and EFs. They were also positively and significantly correlated with EDD and old infarct size (Fig. 8a and b).

4. Discussion

4.1. Injected BM-MNC-derived myocyte-like cells and pericytes—limitation of electron microscopic analysis

Our electron microscopic analysis suggests that very immature (fetal) as well as relatively mature mononuclear cardiomyocytes formed clusters in the infarcted area of the anterior LV myocardium in the hearts of rabbits receiving BM-MNCs following acute MI. These cells differed from cardiomyocytes fused with stem cells which retain the fine ultrastructure and cross-striations of mature cardiomyocytes and are multinuclear [6,12–14]. Each of the myocyte-like cells was positive for DiI particles (a marker of injected BM-MNCs), and DiI particles were observed in pericytes, as well. This finding is consistent with the idea that intravenously injected BM-MNCs are able to transdifferentiate into both myocyte-like cells and pericytes. As BM-MNCs include both hematopoietic and mesenchymal stem cells, it is unclear from which of these cell types the BM-MNC-derived myocyte-like cells are derived.

However, a limitation of electron microscopic analysis is that only very small areas of the tissue samples are actually observed. For that reason, we were unable to precisely determine the total numbers of BM-MNC-derived cells present in infarcted hearts. For the same reason, we cannot rule out the possible existence of cardiomyocytes fused with BM-MNCs. Conversely, negative electron microscopic findings do not imply that the cells are absent.

In the present study, our confocal light microscopic analysis of DiI fluorescence as well as electron microscopic analysis indicated that the incidence of BM-MNC-derived cardiomyocytes was very low in post-MI hearts. However, recent observations reported from several laboratories indicate that following i.v. injection [15], only a very small percentage of cells are actually retained in the heart. Thus, the very small percentage of the regenerated cells is not surprising. However, this observation does not prove that a higher degree of myocyte regeneration cannot be achieved following intramyocardial or intracoronary injection of bone marrow cells. Nor can this observation be extrapolated to imply that bone marrow cell therapy leads to minimal regeneration of cardiomyocytes.

4.2. Up-regulation of SDF-1

Up-regulation of SDF-1 expression was seen in myocardial tissues in the BM-MNC group 7 days post-MI. Given that SDF-1 is able to recruit circulating bone marrow-derived cells into targeted tissues [16–18], this up-regulation may be related to the appearance of BM-MNC-derived cardiac cells.

4.3. Mechanisms of improved LV function and reduced infarct size

A reduction in infarcted area via the formation of less scar tissue could only be supported by an increase in size of the preexisting myocytes and/or the formation of new myocyte, since the total LV area and weight were similar. In the present study, this reduction was equivalent to approximately 10% of the LV area. First, it is clear that the number of regenerated cardiomyocytes within infarcted areas was too small to explain the 10% increase in non-scarred areas. Second, the increase in LV area approximately 10% corresponds to the increase of approximately 3% in the transverse size of cardiomyocytes. Although a significant difference in the transverse size of cardiomyocytes was not observed between the BM-MNC and saline groups in the present study, there is no reliable method of detecting precisely the minimum increase in the transverse size of cardiomyocytes at present. Therefore, the increase in non-scarred areas would be considered to be due to a minimum hypertrophy of preexisting myocytes rather than the regeneration of cardiomyocytes. Further investigation is warranted.

Because the mediators contributing to cardiac development and remodeling are expressed only transiently and may thus be absent from healed and/or newly formed cardiac tissue [19], we assessed their levels at several points post-MI, with the aim of evaluating the causal relationship between changes in cytokine levels and LV function. Expression of TGF-β and MMP-1 is reportedly up-regulated following MI [20–22]. Similarly, in the

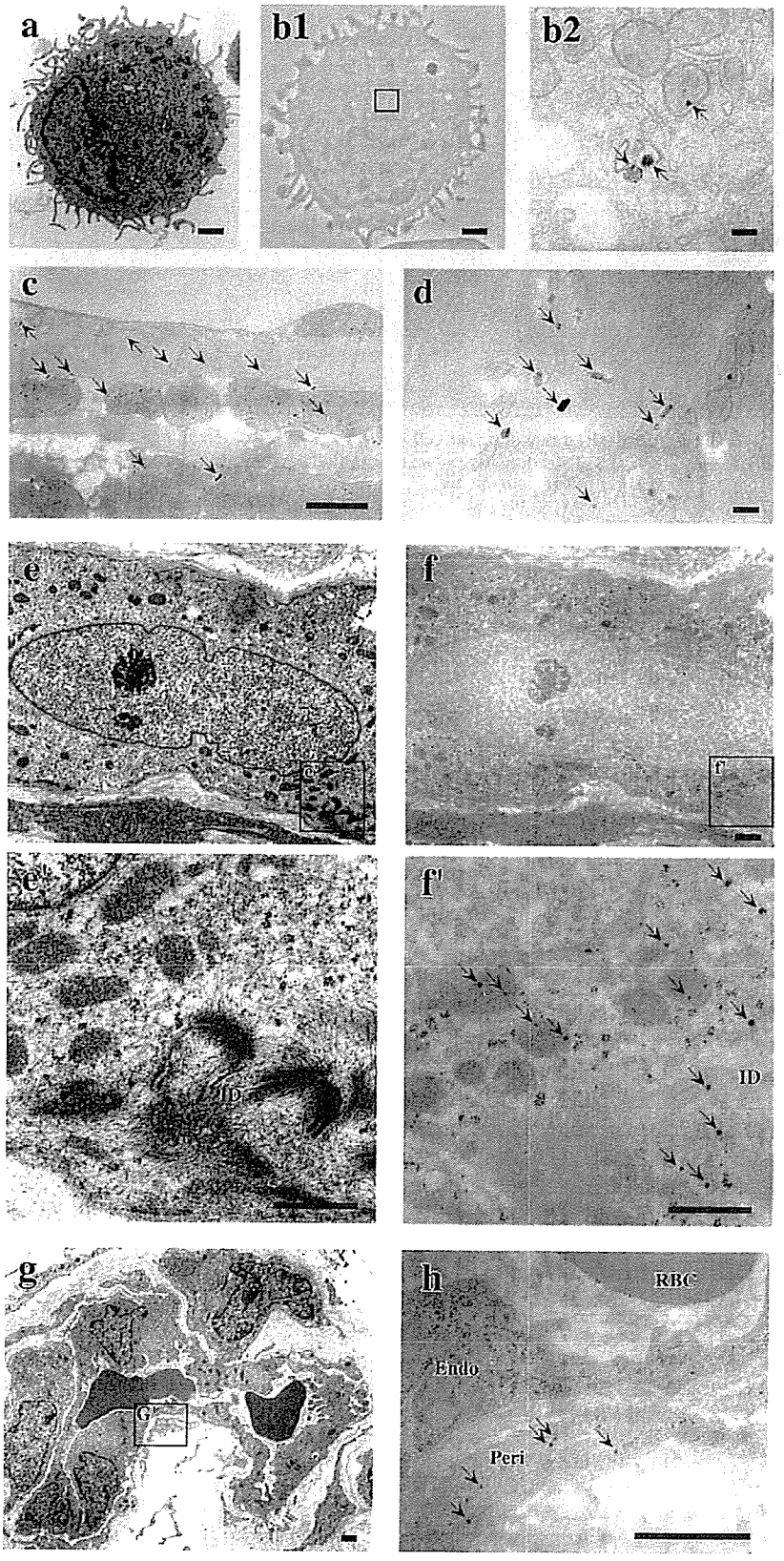
a
b1
b2
c
d
e
ID
f
f'
f'
ID
g
G
h
RBC
Endo
Peri

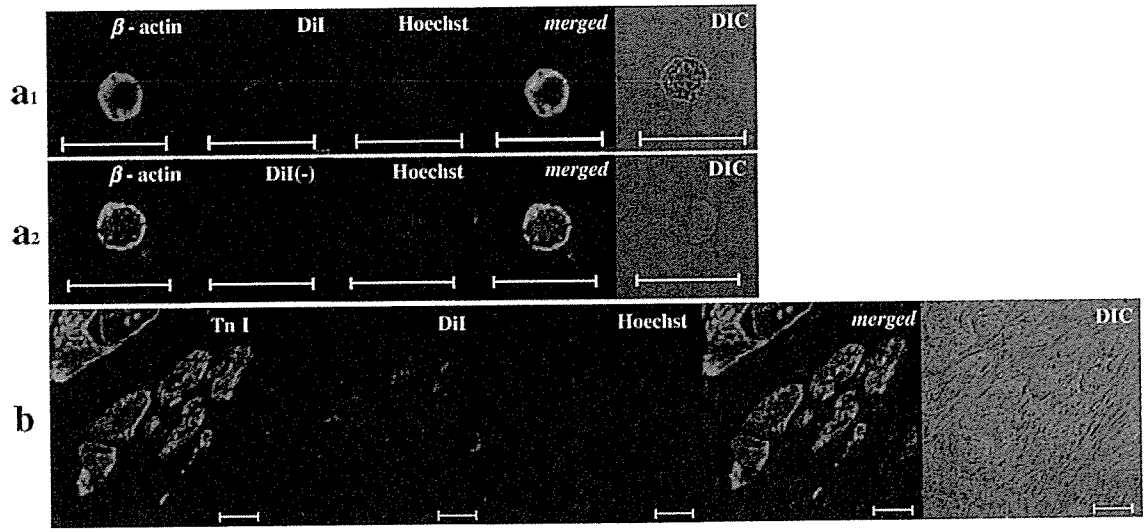

β-actin(*green*): Bone marrow-derived mononuclear cell
DiI(*red*): 1,1'-dioctadecyl-1 to 3,3,3',3'-tetramethylindocarbocyanine perchlorate
Tn I(*green*): Troponin I (a marker of cardiomyocytes)
Hoechst(*blue*): Hoechst33342 (a marker of nuclei)
DIC: Differential interference contrast

Bar: 20μm a (n=3), b(n=6)

Fig. 6. Laser-scanning confocal microscopic findings. Red immunofluorescence is seen in a DiI-labeled BM-MNC (a1) but not in a BM-MNC without DiI labeling (a2). Note the characteristic punctate distribution of DiI in the cytoplasm. (b) Cluster formed by TnI- and DiI-positive BM-MNC-derived cardiomyocytes.

saline group, their expression was up-regulated 7 days and 1 month post-MI. However, we found that this up-regulation was significantly attenuated by administration of BM-MNCs. That the improvement in LV function was not seen in the BM-MNC group until 1 month post-MI means that the down-regulation of cytokines in the BM-MNC group 7 days post-MI preceded the improved LV function. Moreover, the reduction in TGF-β and MMP-1 levels seen 1 month after infarction correlated significantly with the improvement in indicators of LV function (EDD, EF and AWT/PWT ratios), which is consistent with the earlier finding that inhibition of TGF-β or MMP improves cardiac function in failing hearts [21,23,24]. We therefore suggest that the down-regulation of TGF-β and MMP-1 likely contributed to the improved LV function seen in the BM-MNC-treated animals.

Finally, the old infarcts were smaller in the hearts from rabbits administered BM-MNCs than in those from rabbits administered saline, which is indicative of a reduction in the amount of collagen present at the infarct site. This reduction in infarct size is also consistent with the lower levels of TGF-β expressed in BM-MNC hearts, given the ability of TGF-β to induce collagen synthesis. Also, inhibition of apoptosis by a paracrine effect of BMT would be a possible mechanism for the beneficial effect, because the presence has been reported [25].

4.4. Transient increases in vessel density

Generally, vascular regeneration during the chronic stage of MI is enhanced by the injection of BM-MNCs [26]. In the present study, however, the increase in vascular density seen at the subacute stage (7 days post-MI) in the BM-MNC group disappeared during the chronic stage (3 months post-MI). This likely reflects the fact that we used a model of ischemia–reperfusion, which produced moderate infarctions, and differed from the models used in most earlier studies, which involved permanent occlusion

Fig. 5. Electron micrographs showing DiI particles within the ultrastructure. (a) DiI-labeled mononuclear bone marrow cell treated with a conventional electron stain. DiI particles are undetectable, hidden by other cytoplasmic structures. (b1 and b2) Highly magnified micrographs of DiI-labeled, unstained mononuclear bone marrow cells; accumulated DiI particles (arrows) can be clearly seen. (c) DiI-labeled, unstained adult cardiomyocyte in culture; arrows indicate DiI particles. (d) Highly magnified cytoplasm of a DiI-labeled adult cardiomyocyte in culture; DiI particles are indicated by arrows. (e) Conventionally stained myocyte-like cells in the infarcted area 7 days post-MI. (e') Highly magnified micrograph of the boxed portions of panel (e) showing the intercalated disc (ID). (f) Serial section of the myocyte-like cells shown in panel (e) stained for a short period with only lead citrate. (f') Highly magnified photograph of the boxed portions of panel (e) showing abundant DiI particles (arrows). (g) A conventionally stained capillary vessel in the infarcted area 7 days post-MI. (h) Highly magnified photograph of a capillary vessel in a serial, unstained section of the vessel in panel (g). This portion roughly corresponds to the boxed area of panel (g). DiI particles are seen in the pericyte (arrows). ID, intercalated disc; RBC, red blood cell; Endo, endothelial cell; Peri; pericyte. Bars, 0.1 μm in panels (b1), (b2) and (d); 1 μm in the other panels.

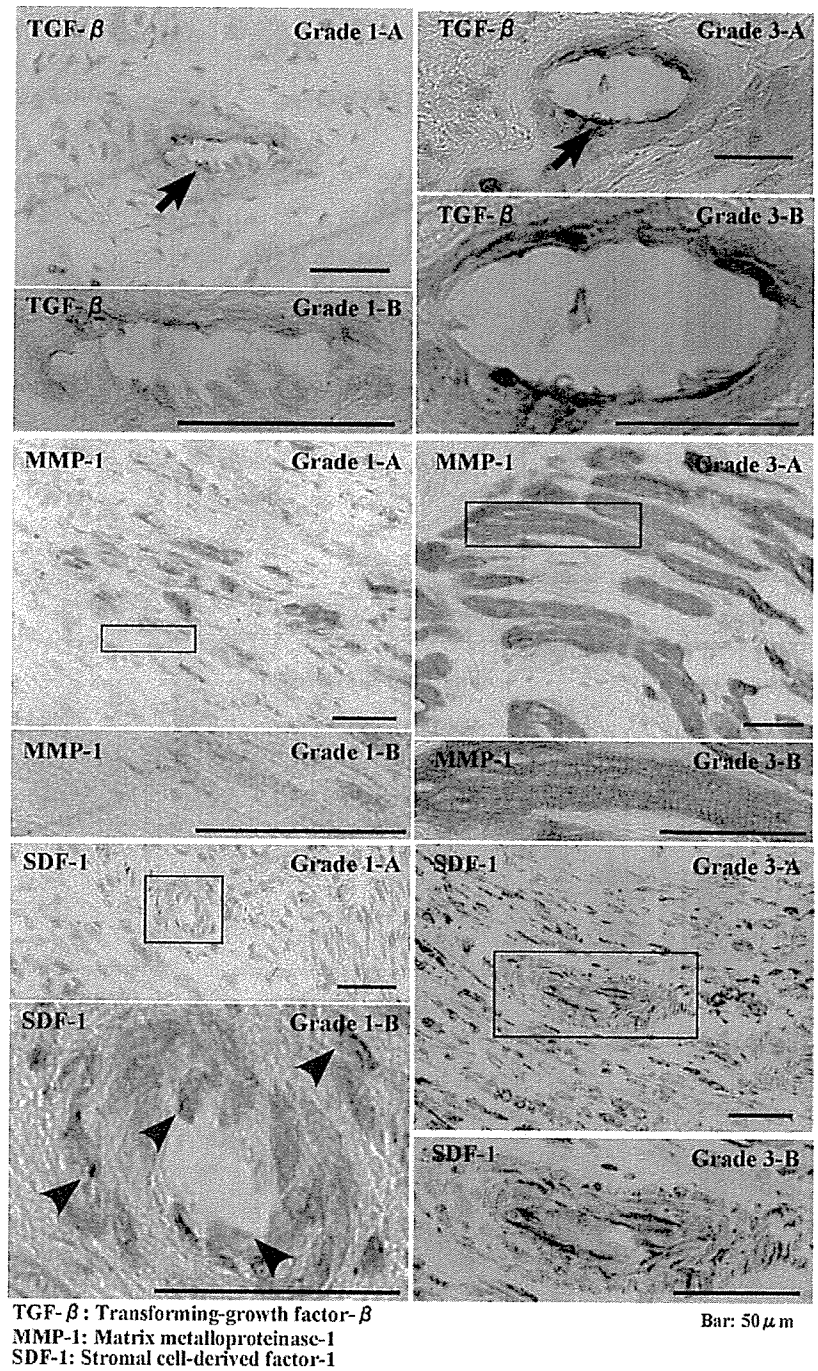

Fig. 7. Immunohistochemical analysis of repair-related cytokines. Immunolabeling of TGF-β and SDF-1 is mainly seen in vascular endothelial cells within infarcted tissues; MMP-1 is detected within cardiomyocytes in the border zone between surviving cardiomyocytes and the infarct. For the morphometric analysis, the expression was assigned a grade of 0 (no expression), 1 (weak expression and focal distribution in <20% of targeted cells), 2 (moderate expression in >20% of targeted cells), or 3 (marked expression and diffuse distribution in >20% of targeted cells) under a high-power field (400×). Grades were assigned to 20–30 high-power fields for each infarcted anterior LV wall. Arrow and arrowheads indicate TGF-β-positive endothelial cells and SDF-1-positive endothelial cells and smooth muscle cells, respectively. Boxed-areas of panel A were highly magnified in panel B.

and produced large infarctions. In the permanent occlusion model, ischemia within the risk areas continues even during the chronic stage; consequently, neovascularization in the form of collaterals is important. On the other hand, in hearts that are reperfused after ischemia, increased neovascularization may be beneficial for the absorption of necrotic tissues and formation of granulation tissue at the subacute stage, but its importance may be reduced at the chronic stage, when the major histological feature is scarring with few cells.